Vessel contrast enhancement in hyperspectral images

Asgeir Bjorgan[a], Martin Denstedt[a], Matija Milanic[a], Lukasz A. Paluchowski[a] and Lise Lyngsnes Randeberg[a]

[a]Norwegian University of Science and Technology, Department of Electronics and Telecommunications, O.S. Bragstads plass 2a, 7034 Trondheim, Norway

ABSTRACT

Imaging of vessel structures can be useful for investigation of endothelial function, angiogenesis and hyper-vascularization. This can be challenging for hyperspectral tissue imaging due to photon scattering and absorption in other parts of the tissue.

Real-time processing techniques for enhancement of vessel contrast in hyperspectral tissue images were investigated. Wavelet processing and an inverse diffusion model were employed, and compared to band ratio metrics and statistical methods. A multiscale vesselness filter was applied for further enhancement.

The results show that vessel structures in hyperspectral images can be enhanced and characterized using a combination of statistical, numerical and more physics informed models.

Keywords: hyperspectral imaging, vasculature, wavelets, optical diagnostics, tissue characterization, diffusion model, inverse model, 3D Monte Carlo

1. INTRODUCTION

High information content in hyperspectral images enables general tissue diagnostics through statistical methods, spectroscopy and optical characterization. The imaging of vessel structures can be useful for investigation of endothelial function, angiogenesis and hyper-vascularization. By using hyperspectral imaging to visualize and monitor vessels, the need for multiple imaging modalities is reduced. It is desired to characterize the vessel structures in terms of oxygenation and depth. Several steps are required before this goal can be met, including vessel contrast enhancement, vessel structure extraction and characterization.

Vessel contrast enhancement in hyperspectral images can be challenging. The pure vessel signal from deeper vessels is in this case obscured by scattering and absorption from other chromophores. These factors make vessels structures appear blurred even in wavelength bands with optimal, natural contrast. A few prior studies exist on vessel enhancement contrast enhancement in hyperspectral or multispectral images of tissue. McCormack et al.[1] applied Beer's law and a Gabor filter[2] for extracting vessels from hyperspectral images of mice. However, these mice were imaged through a imaging window, which would naturally elucidate the vessels. Randeberg et al.[3] extracted vessel structures from human skin using noise-whitened principal component analysis (PCA) (i.e. the Minimum Noise Fraction transform (MNF)). Methods such as PCA will depend on the dynamics of the obtained image statistics. Katrasnik et al.[4] investigated optimal band ratios at longer wavelengths for vessel contrast with the aim of using few wavelengths.

The aim is to use the full wavelength range for consistent vessel contrast enhancement. Preferably should the techniques be applied in real-time due to timing constraints in the clinic.[5,6] This can limit the characterization methods. Due to scattering and absorption, proper characterization of the vessels can require advanced inverse modeling based on photon transport methods. A full reconstruction of the volume for blood vessel characterization will be computationally demanding and will not fulfill the real-time requirements. Vessel contrast enhanced images can be used as *a priori* knowledge of vessel location and used in volumetric reconstruction. The use of simpler models and methods based on this knowledge is investigated.

Further author information: (Send correspondence to A. B.)
A.B.: E-mail: asgeir.bjorgan@iet.ntnu.no

Wavelet techniques are shown to yield suitable vessel contrast enhancement. Initial results regarding determination of oxygenation and depth of the vessels using simple inverse modeling methods are presented. The combined methods will be used to visualize vessel structures in terms of oxygenation and depth.

2. MATERIALS AND METHODS

2.1 Vessel characterization

2.1.1 Vessel contrast enhancement

Wavelet processing techniques have been shown to provide vessel contrast enhanced images.[7] The coefficients resulting from the transform was found to correlate with optical properties. The discrete wavelet transform (DWT) is applied independently to each pixel in the hyperspectral image, along the spectral direction. The mother wavelet $\Psi(x)$ is scaled and moved along the spectrum to yield coefficients at various scales, from various wavelength ranges. The fast wavelet transform (FWT) is a divide-and-conquer algorithm for estimating these coefficients with a complexity of $\mathcal{O}(n \log n)$. The dataset is transformed into approximations and details, where the approximations are iteratively divided into new approximations and details. This is achieved through the use of a low-pass and high-pass filter. A symlet-4 wavelet filter with reflection boundary conditions is used for obtaining vessel enhanced images. A multiscale vesselness filter[8] was applied to the vessel enhanced images.

The MNF transform[9] is used as an example of a more statistical method for obtaining vessel enhanced images. This transform is mainly used for noise removal and compression in hyperspectral images, but can also be used for feature extraction. The image is decomposed into components ranging from high SNR (signal to noise-ratio) to low SNR. These components may sometimes reflect the vessel information, and the transformed image can in such cases show enhanced vessel contrast.

2.1.2 Inverse modeling

Inverse modeling techniques can be used to characterize vessels further beyond the information obtained from contrast enhancement techniques.

Human tissue can be modeled using a multi-layered model with distinct, wavelength dependent absorption coefficients (μ_a), scattering coefficients (μ_s) and anisotropy factors (g) in each layer. Light transport models can be constructed to estimate the amount of back-reflected light for a given skin geometry. Applying these in inverse can yield the optical parameters.

General inverse model A real-time inverse diffusion model for hyperspectral images was developed for a general-purpose use case.[5] The model considers a two-layered skin model in order to simplify the fitting methods and make real-time processing feasible. Different tissue depths are targeted by applying the inverse model to different parts of the diffuse reflectance spectrum. Light in the wavelength range 510-590 nm penetrates more superficially than light in the wavelength range 690-820 nm. Applying the inverse model to these wavelength intervals yields properties down to corresponding penetration depths.

Due to the use of a two-layered model, the derived tissue properties will be smeared out across the geometry, and represent an average value. Vessel properties will be influenced by the surrounding geometry.

The general inverse model can be used as a general contrast enhancement technique, as an increased blood volume fraction would be observed at the location of the vessels.

Vessel targeted inverse model A preliminary inverse model targeted to vessels was developed for estimation of depth, extent and oxygenation.

It was shown by Randeberg et al.[3] that depth information could be extracted from hyperspectral images using a three-layered inverse diffusion model. Dermis was divided in upper and lower dermis with increased blood volume fraction (BVF) in the third layer. Automatic adjustment of this model requires a multi-parameter fitting

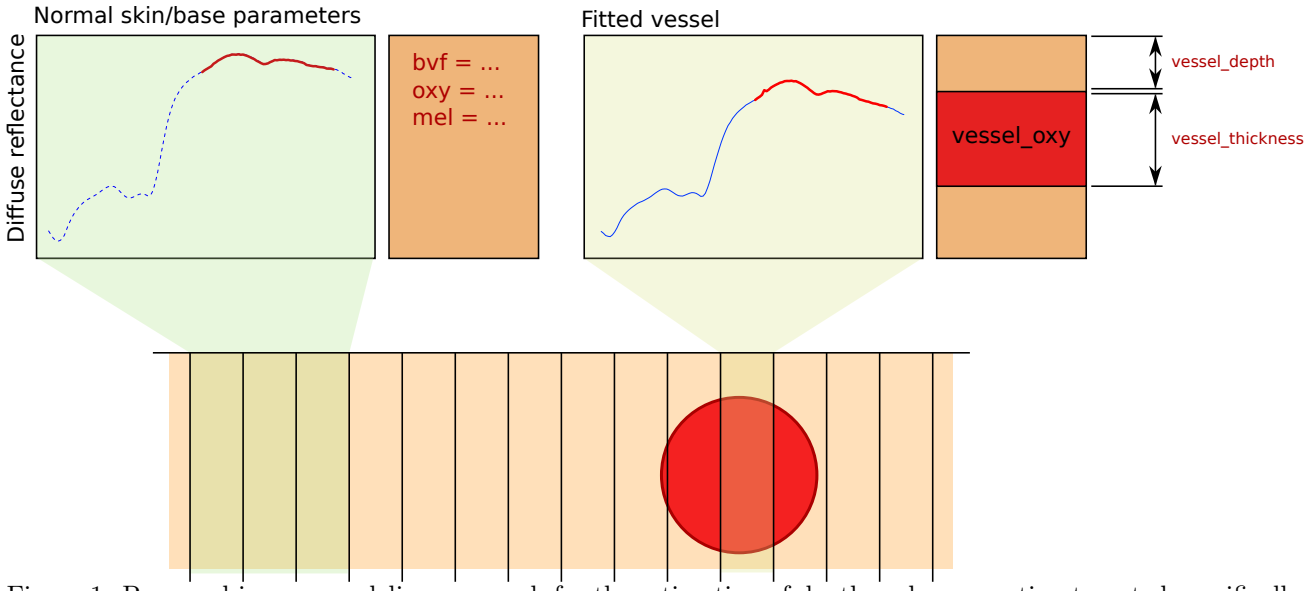

Figure 1: Proposed inverse modeling approach for the estimation of depth and oxygenation targeted specifically to vessels, by exploiting the high spatial resolution of the hyperspectral image.

approach. This might not be sensitive enough to an increase of the BVF in the third layer and can result in an increase in the second layer or affect other parameters.

The approach was adjusted by including a "vesselized" layer in the model. This layer approximates a vessel by fixing its properties to the properties of pure blood (100% BVF, using absorption and scattering properties presented by Friebel et al.[10]). Thickness and depth are adjusted by adjusting the layer depths. In this case a multiparameter fitting approach must be used, where variation of depth and thickness of the vessel can exhibit similarity to an increase of BVF in the other layers. However, the method can be simplified and made more stable with respect to the vessel parameters. The normal skin parameters in the skin layers are fixed to an estimate from a representative area of the skin. It is assumed that the only difference between this selected area and the vessel location is the presence of the vessel. Thus, only the vessel parameters (depth, thickness, oxygenation) are fitted. This fitting method is illustrated in Fig. 1. A one-layered skin model is used for finding a rough estimate of the base skin parameters, while the vessel is approximated as a layer wedged between two base skin layers.

The method requires two spectra, one in the centre of the vessel and one suitably close to the vessel, but without influence from the analyzed vessel or other vessels at similar scale. The initial method does not include automatic extraction of such spectra, but it is expected that they can be obtained using the presented vessel extraction techniques. Thus, the presented method has been tested only on simulated hyperspectral data where the two spectra were chosen manually.

The use of a layer with pure blood, and its laterally infinite extent, has some ramifications on the modeling validity. This will be evaluated.

2.2 Experimental

Hyperspectral images of skin were collected using a push-broom HySpex VNIR-1600 camera (Norsk Elektro Optikk, Lillestrøm, Norway).[11] A healthy, female volunteer (Caucasian, 39 years old) with fair skin (Fitzpatrick skin type I/II) had the volar side of her forearm imaged.

The lens had a focal length of 30 cm. Pixel field of view was approximately 0.4 mrad.[11] Pixel size on the skin surface after magnification using a 30 cm lens was approximately 60 $\times$ 60 μm.

Two linear light sources were used for illumination (Model 2900 Tungsten Halogen, Illumination Technologies). Polarizers were mounted on the camera lens and the light sources (VersaLight polarizer, VLR-100 NIR, 450-1100

nm) in order to avoid specular reflection.

The image was converted to reflectance and corrected for uneven illumination across the field of view using a Spectralon reflectance target (SRT-50-050 Reflectance Target, 12.7 x 12.7 cm, ACAL Bfi Nordic AB, Uppsala). Spectral variations in the specified intensity of the reflectance standard were taken into account in the conversion. The image was denoised using MNF.

The vessel contrast enhancement techniques were applied to the measured hyperspectral data.

2.3 Simulations

Superficial and deep vessels were simulated using a GPU accelerated 3D Monte Carlo model based on the model presented by Milanic et al.[12] Note that tissue and geometry properties are not necessarily physiologically accurate, but should provide the challenge necessary to test the accuracy of the vessel inverse model.

The background tissue was modeled using epidermis, dermis and subcutis, and is based on previous work.[5] Epidermis was set to 0.1 mm. Dermis was set to a thickness of 1.5 mm, and divided in papillary (10% of total dermis thickness) and reticular dermis. Papillary dermis was set to an oxygenation of 50%, while reticular dermis was set to 95%. Both layers had a BVF of 1%. Melanin volume fraction was set to 1%. Tissue optical properties are described in previous works.[5,7]

Two geometries were modeled, each with a voxel size of 10 μm. In the first geometry, a superficial vessel with oxygenation 95% and of radius 300 μm was placed at a depth of 700 μm. The model had a size of 3 mm $\times$ 3 mm. In the second geometry, two deep vessels of radius 950 μm were placed at a depth of 2000 μm. One had oxygenation 95% and the other 70%. The model had a size of 3 mm $\times$ 5mm. The vessels were set to scattering and absorption properties presented by Friebel et al.,[10] and the refraction index presented by Li et al.[13]

The simulated images were averaged along the vessel direction in order to remove noise, and binned into 50 μm size pixels across the vessel direction. The vessel specific inverse diffusion model was applied to the simulated images in order to estimate oxygenation and depth of an embedded layer containing pure blood.

3. RESULTS AND DISCUSSION

Several steps are required for full vessel structure extraction and characterization using hyperspectral imaging. This study presents preliminary methods where vessel structures are extracted using wavelets, and inverse modeling methods are used for estimating depth and oxygenation.

3.1 Contrast enhancement

A sample of wavelet processed images is shown in Fig. 2. Vessels are clearly visualized. A multiscale vesselness filter was applied to iteration 5, detail 6 of the wavelet transform and is shown in Fig. 4.

The third coefficient in the MNF transform can in this case also show vessel enhanced contrast, as seen in Fig. 3(b). However, statistical methods such as MNF will not consistently give enhanced vessel contrast at the same coefficients since the decomposition filters depend on the image statistics. Wavelets always use the same decomposition filters, and the results can be expected to be more consistent.

Investigation of the third component in the MNF transform and the vessel-enhancing coefficients for the wavelet transform show that they primarily work in the wavelength range 600-800 nm with an emphasis on wavelengths around 650 nm. The high vessel contrast may thus be due to the high absorption of deoxyhemoglobin, and the enhanced vessels may primarily be veins.

The images were also inverse modeled using the general inverse diffusion model with the aim of vessel contrast enhancement. The inverse model was applied to the wavelengths 690-820 nm. The wavelength range choice is based on the inverse model's ability to fit it while avoiding crosstalk between deoxyhemoglobin and melanin.[5] Contrasting ability was not taken into account. Thus, while the BVF is heightened or oxygenation lowered in the veins, the resulting contrast will not be superior to other techniques. This is seen in Fig. 5. The contrast is

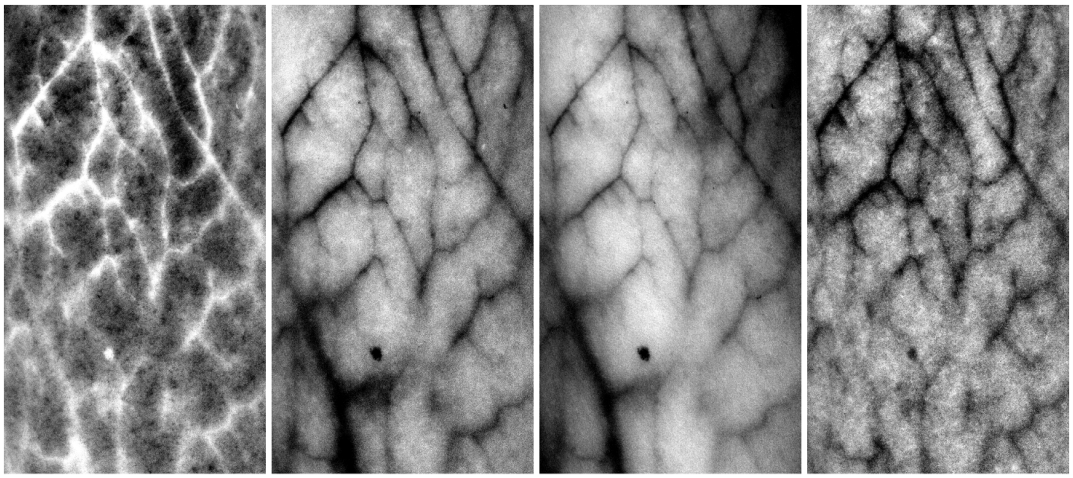

Figure 2: Vessel contrast enhancement using wavelets. The symlet-4 wavelet transform was run along the spectral direction of the hyperspectral image: iteration 5, detail 5 (a), iteration 5, detail 6 (b), iteration 1, detail 35 (c) and iteration 2, detail 17 (d). Results were dynamically scaled.

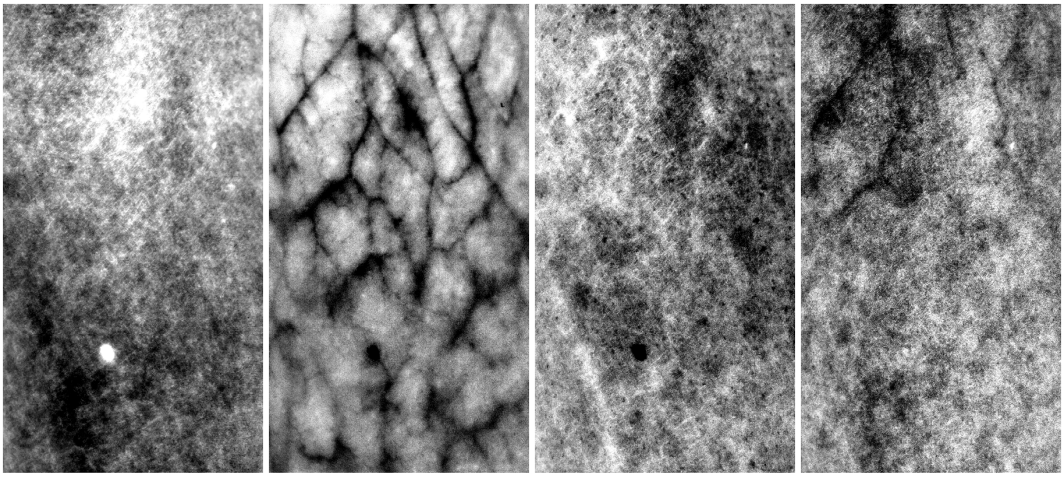

Figure 3: Vessel contrast enhancement using the MNF transform. The second (a), third (b), fourth (c) and fifth (d) band of the MNF transform. Results were dynamically scaled.

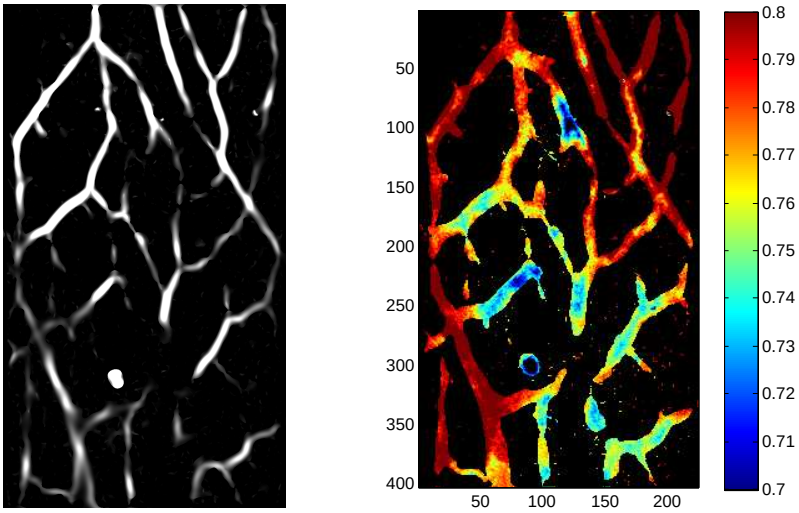

(a) (b)

Figure 4: The multiscale vesselness filter as applied to iteration 5, detail 6 of the wavelet coefficients (a). In (b), oxygenation derived from the general inverse model is applied to the vessels.

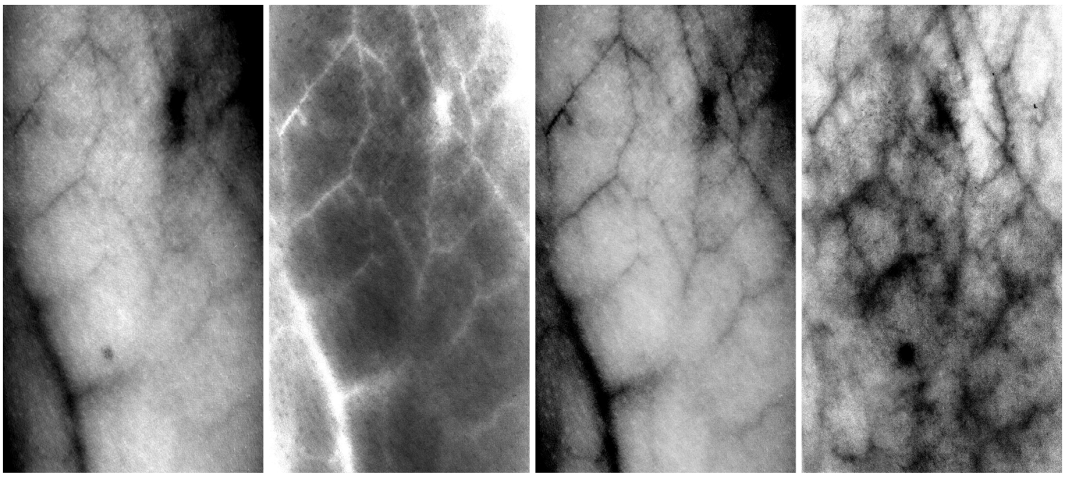

Figure 5: Vessel contrast enhancement using a physics-informed model. Band 133 (a) of a hyperspectral image for comparison, and renormalized inverse modeling results: BVF (b), e^{BVF} (c) and oxygenation (d). The inverse model was fit to the wavelength interval 690-820 nm. Results were dynamically scaled.

not significantly higher than e.g. the band image at a long wavelength. The thin and diffuse appearance of the vessels made it challenging to apply a vessel extraction filter. Different wavelength ranges inspired by the wavelet methods can give better contrast, but will also be influenced by crosstalk and be more prone to misfitting.

The BVF obtained from the physics-informed inverse model has the advantage of not displaying artifacts like moles. This is achieved by having a sufficient melanin separation. The moles are structurally different from normal skin, resulting in different behavior of the reflectance. Wavelets, as a pure mathematical method, shows equal impact from moles as from vasculature, which propagates into a misdetection in the vessel extraction algorithm in Fig. 4.

Denstedt et al.[7] showed that vessel structures could be diminished and moles be enhanced by combining wavelet coefficients. The opposite effect can likely also be achieved in a similar way. Additionally, the approximation coefficient which was used as a BVF map in the same paper showed decreased impact from melanin. The contrast for the smaller vessels were, however, of comparable contrasting ability to the BVF maps obtained using the

diffusion model in our study. Alternatively can the vessel extraction filter be modified to enhance only elongated structures and ignore circular objects like moles.

Of the presented methods, wavelet techniques are more suitable for obtaining vessel enhanced images which can be used for subsequent vesselness filtering.

3.2 Inverse modeling results

3.2.1 General inverse model

The general inverse model was applied to the results obtained from the vesselness filter in Fig. 4. While it generally can give some indication of the oxygenation in the veins, it is limited by the influence from the surrounding geometry. It has been shown[14–17] that the presence of discrete vessels affect the homogeneous assumption in models such as the one used in this study. A vessel distribution should be assumed for more correct derivation of the blood parameters. Initial tests (not shown) showed significant change in the oxygenation for the longer wavelengths when a mean vessel diameter was assumed in the effective blood absorption according to models based on Svaasand et al.[18] Whether the accuracy was improved is currently unknown. More testing is required, where the vessel extraction should be used in the blood vessel distribution assumptions and *a priori* assumptions for the inverse model. Simple averaging of the spectra around the extent of the vessels before inverse modeling can also produce more correct estimates than those gained by estimating oxygenation pixel by pixel. The presented results are a cropped version of the oxygenation in Fig. 5, which are essentially correct with respect to the general perfusion through the skin.[5]

While the general model can be adjusted to get more accurate estimates of the oxygenation, it still cannot give any estimates of the vessel depths, which is also desired to properly discriminate the vessels. Therefore, an inverse model with locatable high amount of blood in the model was tested for vessel depth.

3.2.2 Vessel specific inverse model

The vessel specific inverse model was applied to simulated images of superficial and deep vessels. The superficial vessels had impact on the diffuse reflectance spectrum mainly for the short wavelength range, while the deep vessels had impact on the reflectance spectrum for the longer wavelengths. Therefore, the inverse model was for the superficial vessels applied to the wavelength range 484 nm to 593 nm, while it was applied to 655 nm to 857 nm for the deep vessels.

In order to illustrate the capabilities of the inverse model to reconstruct the vessel volume, the profile of the vessel layer as estimated for each pixel was compared to the actual cross-section of the modeled vessels. Results are shown in Fig. 6a (above) and 6b. The estimated oxygenation for the deep vessels is shown in Fig. 6a (below). The thickness of the derived vesselized layers are negligible outside the extent of the original vessel for the superficial vessel in Fig. 6b, showing ability to reconstruct the vessel volume. The inverse results in Fig. 6a (above) from the deeper vessels show that the inverse modeled vessel layers are thick and non-negligible also outside the extent of the original vessels.

As a first step, these results are promising. Approximate depths and thicknesses can be estimated using a crude model, and it is shown how this estimate varies with distance from the center of the actual vessel. In applying this model, a couple of approximations have ramifications on the validity of the approach.

First, the vessel is approximated as a flat slab, laterally infinite in both directions. The vessel can be approximated to be laterally infinite only in one direction. However, due to a limited penetration depth, the simulated light will only probe at a limited depth both laterally and down into the tissue. With respect to this simplification, the approximation can be said to be more valid in the centre of rather large vessels, subject to the broadening of the light. Fridolin et al.[19] were able develop a homogeneous tissue model with an embedded square vessel using the diffusion approximation. Similar techniques can be valuable for this situation.

Second, a diffusion model is applied. Its validity depends on the isotropy of the radiance within the tissue.[20] This requires a significantly higher scattering coefficient than the absorption coefficient. This is not the case for the absorption and scattering values for pure blood, where the scattering is at best only one order of magnitude

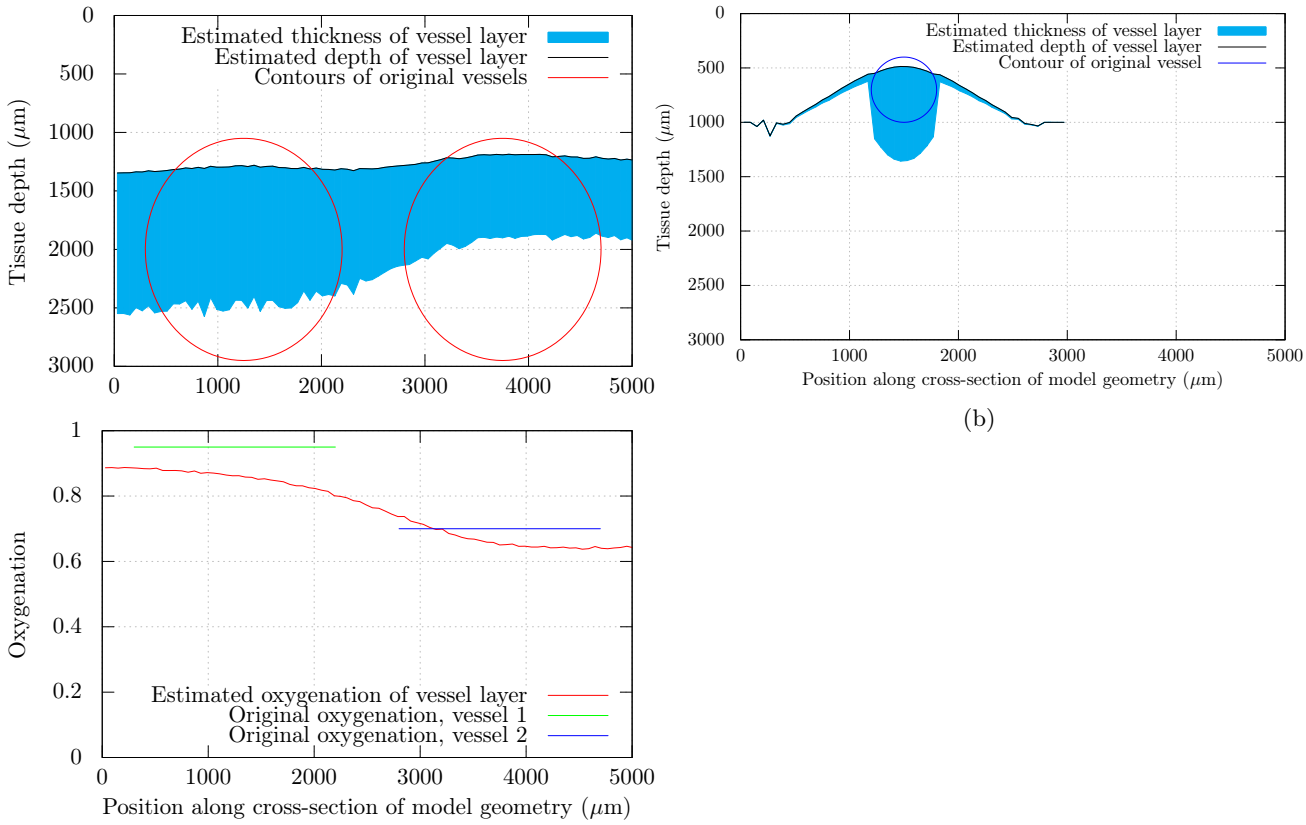

Figure 6: Derived thickness and depth of a layer with pure blood as a function of pixel along the cross-section of the vessel for (a) deep vessels and (b) superficial vessel. The layers were plotted as they would appear within the model, along with the original model of the vessel. The oxygenation for the deep vessels are similarly plotted in (b).

larger than the absorption. The vessel will act as a photon sink in the cases where the penetration depth is less than the diameter of the vessel. The boundary conditions between tissue with low and high albedo can be problematic. Scaling factors[21] or effective absorption coefficients[18] can be used to improve the validity within the vessel.

The approximations would seem to influence the obtained results through either an under-estimation (deep vessels, long wavelengths) or over-estimation (superficial vessels, short wavelengths) of the vessel thickness. However, they do not seem to influence the depth estimate significantly. Even without corrections, the model is likely able to differentiate between vessel depths.

Additionally, the base skin properties are estimated using a homogeneous, one-layered model on normal skin close to the targeted vessel. This can be complicated by the inhomogeneity of human skin. However, though the Monte Carlo model had multiple layers included, this did not seem to influence the results significantly.

The depth estimate obtained using the model, with or without modeling corrections, can be used to estimate the vessel distribution used in the general inverse model to obtain estimates of oxygenation, where the modeling assumptions already are more accurate.

3.3 Real-time feasibility

Both the general inverse modeling method and wavelet method have been implemented in a computationally fast way. Both methods can yield properties in real-time, i.e. within the acquisition time of the hyperspectral

camera. The vessel specific inverse method is more limited, as a multiparameter fitting method has so far been used. Such methods are typically slow, even though the fitted function is fast to evaluate. However, if the number of inverse modeled pixels with the vessels are constrained to a pre-defined number within the extracted vessel structures, the used time can also in this case be constrained to the pure real-time case.

4. CONCLUSION AND FURTHER WORK

Preliminary methods have been shown for obtaining vessel enhanced images and characterizing the vessels using inverse modeling methods. Wavelets have been shown to be a promising technique for vessel contrast enhancement.

Further work will include testing other vessel structure extraction techniques like Gabor wavelet filters[2] on the vessel contrast enhanced images. The vessel structures will be used to obtain spectra from normal skin and spectra from vessels and used for vessel depth estimates. The structures and their estimated depths will be used for calculating vessel distributions and obtain oxygenation estimates.

ACKNOWLEDGMENTS

Thanks to Marc Fournelle for his suggestions to apply the Frangi vesselness filter to wavelet images. MATLAB implementation was obtained from `http://www.mathworks.com/matlabcentral/fileexchange/24409-hessian-based-frangi-vesselness-filter`.

This work is a part of the Iacobus project, `http://www.iacobus-fp7.eu`. Iacobus is supported by the European Commission's 7th RTD Framework Programme Collaborative Project No. 305760.

REFERENCES

[1] D. R. McCormack, A. J. Walsh, W. Sit, C. L. Arteaga, J. Chen, R. S. Cook, and M. C. Skala, "In vivo hyperspectral imaging of microvessel response to trastuzumab treatment in breast cancer xenografts," *Biomed. Opt. Express* **5**(7), pp. 2247–2261 (2014).

[2] H. C. Hendargo, R. Estrada, S. J. Chiu, C. Tomasi, S. Farsiu, and J. A. Izatt, "Automated non-rigid registration and mosaicing for robust imaging of distinct retinal capillary beds using speckle variance optical coherence tomography," *Biomed. Opt. Express* **4**(6), pp. 803–821 (2013).

[3] L. L. Randeberg, E. L. P. Larsen, and L. O. Svaasand, "Hyperspectral imaging of blood perfusion and chromophore distribution in skin," *Proc. SPIE* **7161**, p. 71610C (2009).

[4] J. Katrasnik, M. Buermen, F. Pernus, and B. Likar, "Contrast enhancement of subcutaneous blood vessel images by means of visible and near-infrared hyper-spectral imaging," in *Proc. SPIE* **7259** (2009).

[5] A. Bjorgan, M. Milanic, and L. L. Randeberg, "Estimation of skin optical parameters for real-time hyperspectral imaging applications," *J. Biomed. Opt.* **19**(6) (2014).

[6] A. Bjorgan and L. L. Randeberg, "Real-time noise removal for line-scanning hyperspectral devices using a minimum noise fraction-based approach," *Sensors* **15**(2), pp. 3362–3378 (2015).

[7] M. Denstedt, A. Bjorgan, M. Milanic, and L. L. Randeberg, "Wavelet based feature extraction and visualization in hyperspectral tissue characterization," *Biomed. Opt. Express* **5**(12), pp. 4260–4280 (2014).

[8] A. F. Frangi, W. J. Niessen, K. L. Vincken, and M. A. Viergever, "Multiscale vessel enhancement filtering," in *Proc. Med. Image. Comput. Assist. Interv.* **1496**, pp. 130–137 (1998).

[9] A. A. Green, M. Berman, P. Switzer, and M. D. Craig, "A transform for ordering multispectral data in terms of image quality with implications for noise removal," *IEEE Trans. Geosci. Remote Sensing* **26**(1), pp. 65–74 (1988).

[10] M. Friebel, A. Roggan, G. Mueller, and M. Meinke, "Determination of optical properties of human blood in the spectral range 250 to 1100 nm using monte carlo simulations with hematocrit-dependent effective scattering phase functions," *J. Biomed. Opt.* **11**(3), pp. 034021–1 – 034021–10 (2006).

[11] Hyspex VNIR-1600 Main Specifications, "http://www.hyspex.no/products/hyspex/vnir1600.php." Visited 2014-07-08.

[12] M. Milanic and B. Majaron, "Three-dimensional monte carlo model of pulsed-laser treatment of cutaneous vascular lesions," *J. Biomed. Opt.* **16**(12), pp. 128002–1 – 128002–12 (2011).

[13] H. Li, L. Lin, and S. Xie, "Refractive index of human whole blood with different types in the visible and near-infrared ranges," in *Proc. SPIE* **3914** (2000).

[14] S. L. Jacques, "Optical assessment of cutaneous blood volume depends on the vessel size distribution: a computer simulation study," *J. Biophotonics* **3**(1-2), pp. 75–81 (2010).
[15] R. L. van Veen, W. Verkruysse, and H. J. Sterenborg, "Diffuse-reflectance spectroscopy from 500 to 1060 nm by correction for inhomogeneously distributed absorbers," *Opt. Lett.* **27**(4), pp. 246–8 (2002).
[16] A. Talsma, B. Chance, and R. Graaff, "Corrections for inhomogeneities in biological tissue caused by blood vessels," *J. Opt. Soc. Am. A. Opt. Image Sci. Vis.* **18**(4), pp. 932–9 (2001).
[17] W. Verkruysse, G. W. Lucassen, J. F. de Boer, D. J. Smithies, J. S. Nelson, and M. J. van Gemert, "Modelling light distributions of homogeneous versus discrete absorbers in light irradiated turbid media," *Phys. Med. Biol.* **42**(1), pp. 51–65 (1997).
[18] L. O. Svaasand, E. J. Fiskerstrand, G. Kopstad, L. T. Norvang, E. K. Svaasand, J. S. Nelson, and M. W. Berns, "Therapeutic response during pulsed laser treatment of port-wine stains: dependence on vessel diameter and depth in dermis," *Laser Med Sci* **10**, pp. 235–243 (1995).
[19] I. Fridolin, K. Hansson, and L.-G. Lindberg, "Optical non-invasive technique for vessel imaging: Ii. a simplified photon diffusion analysis," *Phys. Med. Biol.* **45**(12), pp. 3779–3792 (2000).
[20] T. Spott and L. O. Svaasand, "Collimated light sources in the diffusion approximation," *Appl Opt* **39**, pp. 6453–6465 (2000).
[21] R. Zhang, W. Verkruysse, G. Aguilar, and J. S. Nelson, "Comparison of diffusion approximation and monte carlo based finite element models for simulating thermal responses to laser irradiation in discrete vessels," *Phys. Med. Biol.* **50** (2005).